JOURNAL OF COMPUTATIONAL PHYSICS 97, 352–365 (1991)

# Simulation of Ionisation Dynamics and Electron Kinetics

R. MARCHAND AND J. P. MATTE

*INRS-Energie, C.P. 1020, Varennes QC, Canada J3X 1S2*

Received December 12, 1989; revised June 18, 1990

A simple and efficient scheme is presented for simultaneously solving the ionisation dynamics and the electron kinetic equations. The atomic processes accounted for include collisional excitation and ionisation, dielectronic and radiative recombination. The integro-differential equations governing the evolution of the ionisation stages and the electron distribution function are approximated numerically with a Gauss quadrature scheme and finite differences. The result is a set of algebraic nonlinear equations which are solved by iterations. 

## 1. INTRODUCTION

Several key problems of plasma physics require a solution of the particle distribution functions, together with a proper account of certain atomic processes. A precise knowledge of the distribution function is necessary whenever significant deviations from a Maxwell Boltzmann distribution arise. The inclusion of atomic processes is often required because of the contribution to particle and energy balance from these processes. This is the case, for example, in plasmas produced by very short laser pulses, plasmas in or near a strong temperature gradient, or at the edge of magnetically confined plasmas when fueling, recycling or sputtering are important. Methods have already been proposed to solve kinetic equations alone [1–5], or atomic rate equations within a fluid model [6, 7].

In this paper, we present a simple and efficient algorithm for consistently modelling atomic processes within a kinetic simulation code. In short, the method consists of solving the Boltzmann equation for the electron distribution function and the ionization balance equation for the density of charge stages simultaneously and fully implicitly. To this end, the electron distribution function is partitioned into a number of energy groups. The electron kinetic equation, together with the ionisation rate equation then constitute a system of coupled nonlinear equations which are solved by iterations. The method presented is intended for cases where the atomic physics is well approximated by the coronal model, i.e., for low density optically thin plasmas in which multi-step processes and three body recombination are sufficiently small to be neglected or treated perturbatively.

The inclusion of atomic processes to a transport simulation code such as described in Refs. [2, 3], tends to increase the required CPU time significantly. This



0021-9991/91 $3.00

increase is caused by the many ionisation stages and, for each one, the several transitions that need to be accounted for. This burden is particularly heavy if mixtures of several species, or if high $Z$ ions are considered. An efficient procedure for modelling such physics is therefore desirable. The remainder of the paper is organized as follows. In Section 2, we present the general equations, discuss some of their properties and give a simple solution algorithm. Section 3 gives some illustrative numerical results. In these examples, the time splitting technique is used to model inelastic Coulomb collisions between electrons together with atomic processes. Finally, Section 4 contains a summary of our results and some concluding remarks.

## 2. Model Equations

In this section we present ionisation-recombination and electron kinetic equations. We discuss some of their general properties, and propose a simple solution method. For simplicity, we assume a spatially homogeneous and isotropic plasma and consider a single ion species of atomic number $Z$. By using the time splitting technique, the solution algorithm presented here can readily be used in a more general context, accounting, for example, for transport in an inhomogeneous medium.

### A. *Governing Equations*

The density of the various ionisation stages is written as $n_i$, with $i$ varying from 0 for neutral, to $Z$ for fully stripped ions. The equations which describe the ionisation dynamics are assumed to be of the form

$$\begin{aligned}\frac{dn_i}{dt} &= n_{i-1}\int d^3v\, d^3v_1\, d^3v_2\, v\sigma_{i-1}^I(v; v_1, v_2)\, f(v) \\ &\quad - n_i \int d^3v\, d^3v_1\, d^3v_2 \left[ v\sigma_i^I(v; v_1, v_2) + \frac{1}{2} v v_1 \sigma_i^{TR}(v, v_1; v_2)\, f(v_1) \right] f(v) \\ &\quad - n_i \int d^3v\, v\sigma_i^R(v)\, f(v) + n_{i+1}\int d^3v\, v\sigma_{i+1}^R(v)\, f(v) \\ &\quad + n_{i+1}\int d^3v\, d^3v_1\, d^3v_2 \frac{1}{2} v_1 v_2 \sigma_{i+1}^{TR}(v_1, v_2; v)\, f(v_1)\, f(v_2), \end{aligned} \tag{1}$$

where $\sigma_i^I$, $\sigma_i^R$, and $\sigma_i^{TR}$ are the cross sections for collisional ionisation, radiative and dielectronic recombination, and three body recombination respectively, for ionisation stage $i$. In this notation, a semicolon is used to separate the velocity indices of the primary and secondary electrons. For example, $\sigma_i^I(v; v_1, v_2)$ is the differential cross section for ionisation associated with an electron of velocity $v$, producing an ion in stage $i+1$ plus two secondary electrons of velocities $v_1$ and $v_2$;

i.e., $A_i + e(v) \rightarrow A_{i+1} + e(v_1) + e(v_2)$. The terms involving $n_{i-1}$ or $n_{i+1}$ are assumed to vanish identically, when $i = 0$ or $Z$, respectively. We note that Eq. (1) is not of the most general form possible. In particular, it couples the various ionisation stages to adjacent stages only. Also, the rates of ionisation and recombination are assumed to be entirely determined by the density of the various ionisation stages, without explicit reference to the populations of excited states. This approximation is certainly valid in the coronal limit, where the ions are assumed to be in their ground state at the start of any collisional process. More generally, it is also consistent with the coronal radiative model in which the transition rates between the excited states of a given ionisation stage, are assumed to be large compared with the ionisation and recombination rates [8]. In this case, the distribution of excited states is in a quasi steady state for every ion, and it is entirely determined by the plasma distribution function. In this section, we limit our discussion to Eq. (1) because it is generally considered to be adequate for modelling ionisation dynamics in several plasmas of interest.

The equation governing the electron distribution function is

$$\frac{\partial f}{\partial t} = \sum_{i=0}^{Z} n_i \Bigg[ \int d^3v_1 \left[ -v\sigma_i^E(v; v_1) f(v) + v_1 \sigma_i^E(v_1; v) f(v_1) \right] + \int d^3v_1 \, d^3v_2 \Bigg[ -v\sigma_i^I(v; v_1, v_2) f(v) + 2v_1 \sigma_i^I(v_1; v, v_2) f(v_1) - vv_1 \sigma_i^{TR}(v, v_1; v_2) f(v) f(v_1) + \frac{1}{2} v_1 v_2 \sigma_i^{TR}(v_1, v_2; v) f(v_1) f(v_2) \Bigg] - v\sigma_i^R(v) f(v) \Bigg], \tag{2}$$

where $\sigma_i^E(v; v_1)$ is the cross section for collisional excitation (if $v > v_1$) or de-excitation (if $v > v_1$) for ion stage $i$. It is assumed here, without loss of generality, that $\sigma_i^I(v; v_1, v_2)$ and $\sigma_i^{TR}(v_1, v_2; v)$ are symmetric with respect to the interchange of $v_1$ and $v_2$.

B. *Properties*

The general properties of Eqs. (1) have been discussed by Pert [6] when the distribution function (and thus the rates) is given a priori. We are interested here in the properties of the combined set of equations (1) and (2). These are:

(i) Conservation of the number of ions. It follows from Eq. (1), that the total number of ions, $n_0 + \cdots + n_Z$ is constant.

(ii) Conservation of the charge density. With the definition

$$\rho = \sum_{i=1}^{Z} i n_i - \int d^3v \, f(v),$$

it follows that $d\rho/dt = 0$, and Eqs. (1) and (2) therefore conserve the net charge density.

(iii) Decay of the total energy. Equations (1) and (2) contain no energy sources but they do, in general, contain energy sink terms (radiative losses). It follows that the total energy must be a decreasing function of time. This is most easily seen in the absence of super elastic processes, i.e., if $\sigma_i^E(v_1; v_2) = 0$ whenever $v_1 < v_2$. The total plasma energy is then defined as

$$U = \sum_{i=1}^{Z} n_i \alpha_i + \int d^3v \, \tfrac{1}{2} m v^2 f(v), \tag{3}$$

with the cumulative ionisation energies $\alpha_i$ defined recursively in terms of the ionisation potentials $\chi_i$ as $\alpha_0 = 0$, and $\alpha_i = \alpha_{i-1} + \chi_{i-1}$ for $i \geqslant 1$. In the presence of super elastic processes, the total energy (including the excitation energy) can also be shown to be a decreasing function of time.

Properties (i) and (ii) are important conservation properties which must be preserved in the approximate numerical solution scheme. This is particularly true of charge conservation since large spurious electric fields could arise in spatially non-homogeneous simulations if the charge failed to be conserved. As a consequence of property (iii), the only steady state solution of Eqs. (1) and (2) is for a cold neutral gas. Nontrivial steady state solutions exist if electron–electron collisions are taken into account to couple the various energy groups of $f$ and if an energy source term is included in Eq. (2). Such a term could be associated, for example, with energy transport, or local heating. We note finally that, while the total energy is, in general, a decreasing function of time, the temperature of the plasma may be increasing. This can happen in a recombining plasma, because of the larger recombination cross section associated with the less energetic particles in radiative recombination.

C. *Solution Algorithm*

In order to solve Eqs. (1) and (2), we approximate time derivatives by finite differences,

$$\frac{dg}{dt} \simeq \frac{g^+ - g^-}{\Delta t} \tag{4}$$

for all dynamic variables $g$. The superscripts $+$ and $-$ refer to the variable after and before time step $\Delta t$, respectively. Velocity space is limited to a finite interval $0 \leqslant v \leqslant v_{\max}$. It is then partitioned into $N$ subintervals with boundaries $v_0 = 0 < v_1 < \cdots < v_N = v_{\max}$. The distribution function is represented by an $N$ component vector $(f_1, ..., f_N)$, associated with the $N$ velocity (or energy) subintervals. The velocity integrals are approximated by quadrature schemes of the form

$$\int d^3v \, f(v) \simeq \sum_{j=1}^{N} w_j f_j, \tag{5}$$

where the weight coefficients $w_j$ are functions of the velocities $v_j$ satisfying the consistency condition

$$\lim_{\max(\Delta v_j)\to 0} \sum_{j=1}^{N} w_j f_j = 4\pi \int_0^{v_{\max}} dv\, v^2 f(v) \tag{6}$$

for any integrable function $f$. This condition is not very restrictive in that it may be satisfied by a wide choice of partitions $\{v_i\}$ and weights $\{w_i\}$. A further restriction is often imposed by requiring consistency with the other numerical solution algorithms used in the simulation. For example, if both atomic processes and Coulomb collisions need to be accounted for, it is important that the velocity integration scheme used in Eq. (5) be consistent with the conservation properties of the collision operator. For example, if Coulomb collisions are treated in the Fokker–Planck approximation and if the resulting equation is advanced in time with Cooper and Chang's implicit scheme [9], this implies that $w_i = v_{i-1/2}^2 (v_i - v_{i-1})$, with $v_{i-1/2} = (v_{i-1} + v_i)/2$. With these approximations for the time derivatives and the velocity integrals, Eqs. (1) and (2) yield a set of $N+Z+1$ coupled nonlinear equations in the unknown variables $n_i^+$ and $f_j^+$, of the form

$$\begin{aligned}
&-n_{i-1}^+ \sum_{jkl} \tilde{v}_j \sigma_{i-1}^I(j;k,l)\, f_j^+ w_j w_k w_l \\
&\quad + n_i^+ \left[ \frac{1}{\Delta t} + \sum_{jkl} \left[ \tilde{v}_j \sigma_i^I(j;k,l) + \frac{1}{2} \tilde{v}_j \tilde{v}_k \sigma_i^{TR}(j,k;l)\, f_k^+ \right] f_j^+ w_j w_k w_l \right. \\
&\quad \left. + \sum_j \tilde{v}_j \sigma_i^R(j)\, f_j^+ w_j \right] \\
&\quad - n_{i+1}^+ \left[ \sum_j \tilde{v}_j \sigma_{i+1}^R(j)\, f_j^+ w_j + \sum_{jkl} \frac{1}{2} \tilde{v}_j \tilde{v}_k \sigma_{i+1}^{TR}(j,k;l)\, f_j^+ f_k^+ w_j w_k w_l \right] \\
&= \frac{1}{\Delta t} n_i^-
\end{aligned} \tag{7}$$

for $i = 0, \ldots, Z$, and

$$\begin{aligned}
&f_j^+ \left\{ \frac{1}{\Delta t} + \sum_i n_i^+ \left[ \sum_k \tilde{v}_j \sigma_i^E(j;k) w_k + \sum_{kl} \tilde{v}_j \sigma_i^I(j;k,l)\, w_k w_l \right. \right. \\
&\quad \left. \left. + \sum_{k>j} \sum_l \tilde{v}_j \tilde{v}_k \sigma_i^{TR}(j,k;l)\, f_k^+ w_k w_l + \tilde{v}_j \sigma_i^R(j) \right] \right\} \\
&\quad - \sum_i n_i^+ \left[ \sum_{k>j} \tilde{v}_k \sigma_i^E(k;j)\, f_k^+ w_k + \sum_{k>j} \sum_l 2\tilde{v}_k \sigma_i^I(k;j,l)\, f_k^+ w_k w_l \right] \\
&= \frac{1}{\Delta t} f_j^- + \sum_i n_i^+ \left[ \sum_{k<j} \tilde{v}_k \sigma_i^E(k;j)\, f_k^+ w_k + \sum_{k<j} \sum_l 2\tilde{v}_k \sigma_i^I(k;j,l)\, f_k^+ w_k w_l \right. \\
&\quad \left. - \sum_{k \leqslant j} \sum_l \tilde{v}_j \tilde{v}_k \sigma_i^{TR}(j,k;l)\, f_k^+ w_k w_l + \sum_{kl} \frac{1}{2} \tilde{v}_k \tilde{v}_l \sigma_i^{TR}(k,l;j)\, f_k^+ f_l^+ w_k w_l \right]
\end{aligned} \tag{8}$$

for $j=1, ..., N$. The velocities $\tilde{v}_j$ must be defined so as to be representative of the subintervals $[v_{j-1}, v_j]$. In the following, we assume $v_j=(v_{j-1}+v_j)/2$. For brevity, the velocities $\tilde{v}_j$ appearing as arguments of the differential cross sections are replaced by their subscript $j$. Unless otherwise stated, the summations extend over the entire range possible, i.e., from 0 to $Z$ for ionisation stages and from 1 to $N$ for the components of the distribution function. Equation (8) has been written so that the left-hand side is characterized by an upper triangular operator, while the right side (excepting the first term) is mostly lower triangular with zero diagonal. We note that the second summation on the right-hand side of Eq. (8) accounts for ionisation from auto ionizing states. The last summation, with $\tilde{v}_k^2+\tilde{v}_l^2<\tilde{v}_j^2$ accounts for the inverse process, that is, recombination into auto ionizing states.

(i) The coronal limit. It is interesting to note that, in the absence of three-body recombination and super elastic collisions; i.e., if $\sigma_i^E(k; j)=0$, whenever $\tilde{v}_k<\tilde{v}_j$, and $\sigma_i^I(k; j, l)=0$, whenever $\tilde{v}_k^2<\tilde{v}_j^2+\tilde{v}_l^2$, the summations on the right-hand side of Eq. (8) vanish, and the system of Eqs. (8) becomes linear upper triangular in $f^+$. This suggests a two-stage iterative solution for Eqs. (7) and (8), in which Eq. (8) is first solved for $f^+$ for an assumed distribution of ionisation stages $n_i^+$. Because of the triangular structure of the matrix equation for $f^+$, this can be done directly, in a single descending sweep from $j=N$ to $j=1$. In the second stage, the tridiagonal set of Eqs. (7) is solved for $n_i^+$, assuming the $f_j^+$ found in the first stage. These $n^+$ are substituted back in Eq. (8), and the procedure is repeated until convergence. Specifically, we rewrite Eqs. (7) and (8) as

$$\sum_{jk} T_{ik,j} f_j^+ n_k^+ = \frac{n_i^-}{\Delta t} \tag{9}$$

and

$$\sum_{ik} U_{i,jk} n_i^+ f_k^+ = \frac{f_j^-}{\Delta t}, \tag{10}$$

where $T_{ik,j}$ is a tridiagonal operator for $n_i$ and $U_{i,jk}$ is an upper triangular operator for $f_j$. In these expressions, a comma is used to separate indices associated with charge stages and the components of the distribution function. Because Eqs. (9) and (10) are nonlinear, they need to be solved by iterations. Let $f_j^0$ and $n_i^0$ be the starting values for $f$ and $n$ at a given time step. In practice, $f_j^0=f_j^-$ and $n_i^0=n_j^-$ prove to be a convenient choice. The components $f^\alpha$ and $n^\alpha$ at iteration $\alpha$ are defined recursively by

$$\sum_{ik} U_{i,jk} n_i^\alpha f_k^{\alpha+1} = \frac{f_j^-}{\Delta t} \tag{11}$$

and

$$\sum_{jk} T_{ik,j} f_j^{\alpha+1} n_k^{\alpha+1} = \frac{n_i^-}{\Delta t}. \tag{12}$$

These iterations must be repeated until convergence. A detailed discussion of convergence is given in Section 3C.

(ii) Extension to non-coronal plasmas. The solution procedure presented in the previous paragraph can readily be extended to account for super elastic processes and three-body recombination, provided that these effects are sufficiently small to be treated perturbatively. This can be done, for example, by rewriting Eq. (8) in the form

$$\sum_{ik} U_{i,jk} n_i^+ f_k^+ + \sum_{il} \sum_{k>j} B_{i,jkl} n_i^+ f_j^+ f_k^+ = \frac{f_j^-}{\Delta t} + \sum_{ik} L_{i,jk} n_i^+ f_k^+ - \sum_{il} \sum_{k \leqslant j} B_{i,jkl} n_i^+ f_j^+ f_k^+ + \frac{1}{2} \sum_{ikl} B_{i,klj} n_i^+ f_k^+ f_l^+, \quad (13)$$

where $U_{i,jk}$ is the same operator as in Eq. (10), $B_{i,jkl} = \tilde{v}_j \tilde{v}_k \sigma_i^{TR}(j, k; l) w_j w_k$ acounts for three body recombination, and $L_{i,jk}$ is a lower triangular operator (with zero diagonal) for $f_j$ which accounts for all super elastic processes which are linear in $f$. We note that if $n_i^+$ were known and if all the summations in the right-hand side of Eq. (13) vanished, a solution for $f^+$ could be found directly in a single descending sweep for $j = N$ to $j = 1$. This suggests a similar iterative solution as for the coronal limit, with the exeption that Eq. (11) is now replaced by

$$\sum_{ik} U_{i,jk} n_i^\alpha f_k^{\alpha+1} + \sum_{il} \sum_{k>j} B_{i,jkl} n_i^\alpha f_j^{\alpha+1} f_k^{\alpha+1} = \frac{f_j^-}{\Delta t} + \sum_{ik} L_{i,jk} n_i^\alpha f_k^\alpha - \sum_{il} \sum_{k \leqslant j} B_{i,jk} n_i^\alpha f_j^\alpha f_k^\alpha + \sum_{ikl} B_{i,klj} n_i^\alpha f_k^\alpha f_l^\alpha. \quad (14)$$

We note that this extension of the solution algorithm is proposed here without verification; the only simulations made so far have assumed the coronal limit.

## 3. Example Results and Discussion

The solution algorithm presented in the previous section has been applied to model the ionisation and recombination in a low density carbon plasma in the coronal approximation. The ionisation cross sections are computed as a function of energy from analytic fits [10]. The cross sections for excitation, radiative, and dielectronic recombination are such that they reproduce the corresponding rates used in the MIST code [11] for a Maxwellian electron distribution function. The accuracy of these empirical cross sections may be questionable, particularly for low ionisation stages. The solution method, however, is not sensitive to the particular atomic model selected, and it could just as well be used with a more complete and accurate set of cross sections. In the calculation of the excitation and recombination cross sections, the energy levels are calculated approximately in the screened

hydrogenic ion model [12, 13]. In the simulations considered here, Coulomb collisions are accounted for, together with atomic processes, using a time splitting technique. That is, at each time step, atomic processes and collisions are treated separately in two distinct steps. Collisions are treated in the Fokker–Planck approximation [14] and the associated equations are solved using Chang and Cooper's implicit scheme [9]. We note that because of the weak density and temperature dependence of the collisional interruption term appearing in the empirical cross sections for dielectronic recombination, the cross sections and much of the calculations involved in the matrix $U$ need not be repeated at each iteration step. Two cases are considered. The first is for a rapidly ionizing plasma while the second is for a recombining plasma. In each case, a solution is first found with a relatively large time step, which allows appreciable variations ($\sim 10\%$) in the electron mean energy at each step. In order to assess the accuracy of this solution, a more accurate simulation is then made with a much smaller time step. All simulations are carried with an 80-point mesh, uniform in velocity, extending from 0 to four times the initial electron thermal velocity, $v_{\text{th}} = (2T/m_e)^{1/2}$.

### A. *Ionizing Plasma*

We consider a plasma made initially of 100% singly ionized carbon ions of density $n_C = 10^{18}\text{m}^{-3}$, with an electron temperature $T_e = 100\text{eV}$. For these parameters, the ionisation and Coulomb collision [15] time scales are approximately equal, $\tau_{\text{ionis}} \sim \tau_{\text{col}}$. In order to test the convergence of the solution algorithm, we choose a sufficiently long time step for macroscopic quantities to vary significantly during a single time step. Specifically, $\Delta t$ is one-sixteenth of the reciprocal of the initial ionisation rate for CII. For the parameters assumed here, this is $\Delta t = 2.25\mu\text{s}$. The simulation was carried until the electron temperature had decreased by

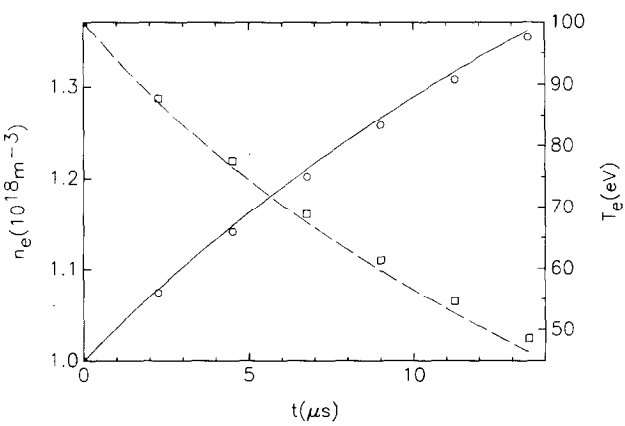


FIG. 1. Electron density and temperature computed as a function of time for the rapidly ionizing plasma considered in Section 3A. The simulation results obtained with the larger time step $\Delta t = 2.25\mu\text{s}$ are shown by the circles for the density and the squares for the temperature. The corresponding accurate solutions obtained with a smaller time step are shown with the solid and dashed lines respectively.

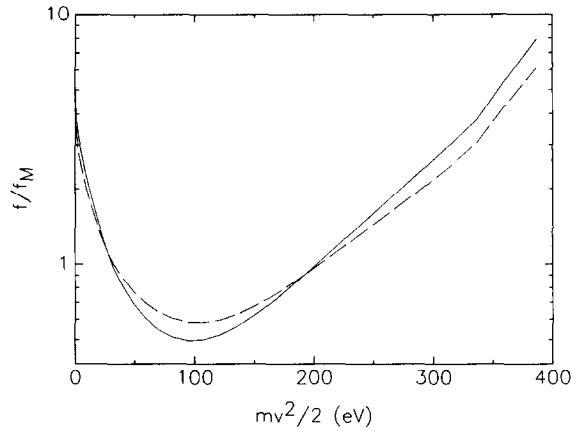


FIG. 2. Ratio of the actual electron distribution function to a Maxwellian distribution with the same density and temperature, computed at $t = 13.5\mu s$. The dashed line was calculated from the simulation using $\Delta t = 2.25\mu s$, while the solid line was computed from the accurate simulation.

approximately a factor two. The time step used in this simulation is somewhat smaller than the electron–electron Coulomb collision time [15], $\Delta t/\tau_{col} \simeq 0.06$. We note that the electron distribution function which results is, in general, not Maxwellian. The temperature considered here is defined such that $3n_e T_e/2$ is the mean electron thermal energy. The results are shown in Fig. 1 for the electron temperature (squares) and density (circles) as a function of time. Figure 2 (dashed) shows the ratio $f/f_M$ of the final electron distribution function to a Maxwellian distribution with the same density and temperature. The entire simulation was completed in six time steps and the temperature is found to vary by approximately 10% at each time step. Only three iterations were required, to conserve the net charge density to one part in $10^8$ throughout. Also shown in these figures are the accurate electron density (solid) and temperature (dashed), and the ratio $f/f_M$ (solid) obtained with a much smaller time step. By comparison, the simulation done with $\Delta t = 2.25\mu s$ is seen to be accurate within approximately 3%.

B. *Recombining Plasma*

We now consider a plasma made initially of 100% fully ionized carbon of density $n_C = 10^{21} m^{-3}$, with an electron temperature $T_e = 100 eV$. According to the empirical model, the initial radiative recombination rate is $\nu_r = 1083 s^{-1}$. The Coulomb collision time is estimated to be $\tau_{col} \simeq 46 ns$. This is smaller than the recombination time ($\nu_r^{-1}$) by a factor approximately $2 \times 10^4$. The simulation was done with a time step $\Delta t = 10\mu s$ until the electron temperature decreased by approximately a factor of 2. The time step considered here is approximately one-hundredth of the reciprocal of the initial recombination rate. It is, however, much larger than the electron–electron Coulomb collision time ($\Delta t/\tau_{col} \simeq 217$). The results are shown in Fig. 3 for the electron density (circles) and temperature (squares), and in Fig. 4 for the distribution

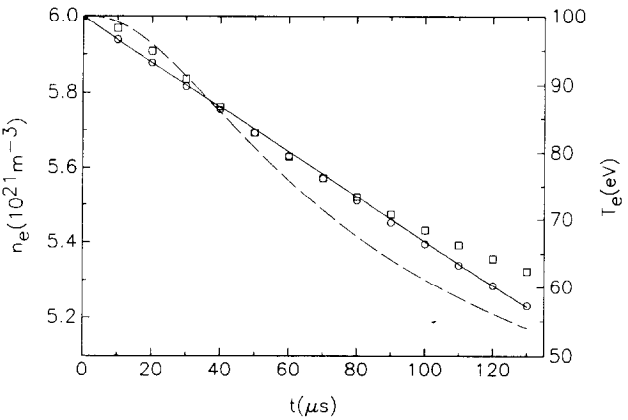


FIG. 3. Electron density and temperature computed as a function of time for the recombining plasma considered in Section 3B. The simulation results obtained with the larger time step $\Delta t = 10\mu s$ are shown by circles for the density and the squares for the temperature. The corresponding accurate solutions obtained with a smaller time step are shown with the solid and dashed lines respectively.

of ionisation stages (circles). As in the first case, this simulation was repeated with a smaller time step to yield an accurate solution. In the simulation done with $\Delta t = 10\mu s$, the number of iterations required to conserve charge density to one part in $10^8$ varied between 4 and 5. The electron density and distribution of ionisation stages calculated with the larger time step are seen to be accurate within 4%. The error in the temperature, however, is somewhat larger. In particular, the final temperature is overestimated by approximately 14% when $\Delta t = 10\mu s$.

The difficulty in this case is caused by the use of a time splitting technique with

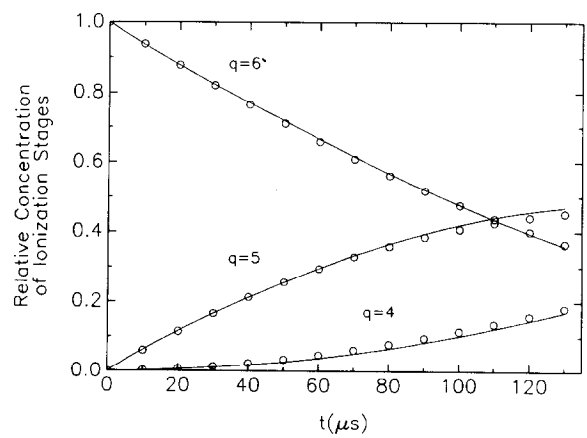


FIG. 4. Distribution of the three main charge stages as a function of time, for the recombining plasma of Section 3B. The circles result from the simulation done with $\Delta t = 10\mu s$. The solid lines represent the accurate solution obtained with a much smaller time step.

two processes characterized by very different time scales. During the Boltzmann or atomic physics step, the plasma is formally treated as collisionless and the electron distribution function is allowed to deviate from a Maxwellian. During the collision or Fokker–Planck step, however, the strong electron–electron collisions restore the electron distribution function back to an almost exact Maxwellian. In reality, collisions and atomic processes are taking place simultaneously and, because of the strong collisions, the electron distribution function should never be allowed to deviate significantly from a Maxwellian. This problem can be corrected by choosing a sufficiently small time step to prevent significant departures from a Maxwellian distribution. This is how the accurate solutions (solid and dashed) were obtained in Figs. 3 and 4. An alternate and numerically more satisfactory solution would be to account for both collisions and atomic processes simultaneously and fully implicitly. This generalization of the solution algorithm is beyond the scope of the present article. In short, because the Fokker–Planck operator is nonlinear in $f$, it would involve solving a set of coupled nonlinear equations for the $f_j$.

C. *Convergence*

The iterative procedure described in Section 2C yields, if it converges, an exact solution to Eqs. (7) and (8) in the limit when $\alpha$ goes to infinity. In practice, only a finite number of iterations can be made, and it is necessary to find a criterion for determining when the approximate solution $f^\alpha$, $n^\alpha$ is sufficiently close to the exact solution. We now consider three such convergence criteria for the two cases considered in the previous paragraph. In this discussion, we restrict our attention to Eqs. (11) and (12) for the coronal limit.

A good convergence criterion is one which directly assesses how well the various equations are satisfied. The first two citeria considered are constructed to assess how well Eqs. (9) and (10) are satisfied at each iteration. Specifically, we define

$$\varepsilon_1^\alpha = \frac{\sum_j (\sum_{jk} U_{i,jk} n_i^{\alpha-1} f_k^{\alpha-1} - f_j^-/\Delta t)^2 w_j^2}{\sum_j (f_j^- w_j/\Delta t)^2} \tag{15}$$

$$\varepsilon_2^\alpha = \frac{\sum_i (\sum_{jk} T_{ik,j} f_j^\alpha w_j n_k^{\alpha-1} - n_i^-/\Delta t)^2}{\sum_i (n_i^-/\Delta t)^2}. \tag{16}$$

By definition of $f^\alpha$ in Eq. (11), $\varepsilon_1^\alpha$ vanishes if $f^{\alpha-1}$ is replaced by $f^\alpha$ in Eq. (15). Similarly, $\varepsilon_2^\alpha$ vanishes if $n^{\alpha-1}$ is replaced by $n^\alpha$ in Eq. (16). Thus, at convergence, when $f^\alpha$ and $n^\alpha$ approach $f^{\alpha-1}$ and $n^{\alpha-1}$, both $\varepsilon_1^\alpha$ and $\varepsilon_2^\alpha$ must approach zero. The parameters $\varepsilon_1^\alpha$ and $\varepsilon_2^\alpha$ indicate how well the systems of Eqs. (10) (with $j = 1, N$) and (9) (with $i = 0, Z$) are satisfied globally.

We consider a third convergence criterion, based on the conservation properties of the system of Eqs. (9) and (10). We have seen in Section 2 that Eqs. (7) and (8) conserve the net electrical charge. It can also be verified that the finite difference form of these equations, Eqs. (9) and (10), also conserves the net charge density. The non-converged solution, $f^\alpha$ and $n^\alpha$, on the other hand, do not conserve charge, in general, which suggests an ad hoc convergence criterion based on charge

conservation. This criterion is simple to evaluate, and it involves quantities which need to be calculated anyway. Assuming a unit electron charge for simplicity, we define the electron and ion charge density at iteration step $\alpha$ as

$$\rho_{\text{ion}}^{\alpha} = \sum_i i n_i^{\alpha} \tag{17}$$

and

$$\rho_{\text{el}}^{\alpha} = -\sum_j f_j^{\alpha} w_j. \tag{18}$$

The third convergence criterion is then defined as

$$\varepsilon_3^{\alpha} = \left| \frac{(\rho_{\text{ion}}^{\alpha} + \rho_{\text{el}}^{\alpha}) - (\rho_{\text{ion}}^{0} + \rho_{\text{el}}^{0})}{\rho_{\text{el}}^{0}} \right|. \tag{19}$$

As an example, the values of $\varepsilon$ computed during the first time step of simulations *A* and *B* are shown in Fig. 5. For a given simulation, the rate of convergence is seen to be nearly the same for all three $\varepsilon$. Also, $\varepsilon_3$ is always the smallest, and $\varepsilon_1$, the largest of the three $\varepsilon$, the ratio $\varepsilon_1/\varepsilon_3$ being nearly independent of the iteration step. These results suggest that charge conservation $\varepsilon_3$ may be used as a practical ad hoc conservation criterion.

The simulations considered here show a relatively fast convergence to the solution. The iterative solution presented in Section 2 is generally found to be robust and to converge, even in cases where the time step is well in excess of what would

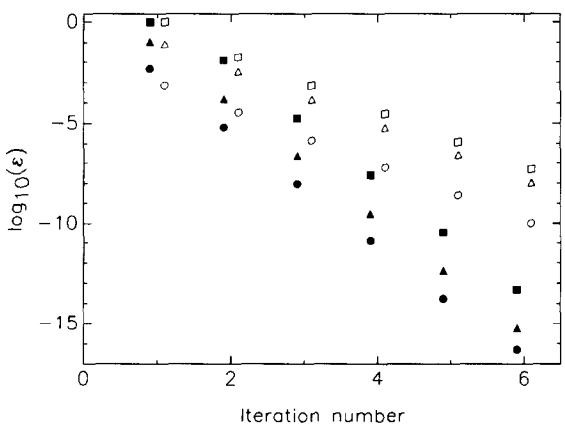


FIG. 5. Convergence criteria computed at each iteration step during the first time step of simulations *A* and *B* of Section 3; $\varepsilon_1$ and $\varepsilon_2$ are represented by squares and triangles, respectively. The relative charge nonconservation $\varepsilon_3$ is shown by circles. The values of $\varepsilon$ computed for the ionising plasma (case *A* in Section 4) are represented by closed symbols while those computed for the recombining plasma (case *B*) are represented by open symbols.

normally be considered acceptable for a meaningful solution. For example, if the time step used in case B (which exhibits the slower convergence) is multiplied by a factor 10 ($\Delta t \to 100\mu s$), both $\varepsilon_1$ and $\varepsilon_2$ are still less than $2 \times 10^{-7}$, and $\varepsilon_3$ is less than $10^{-8}$ after 10 iterations in the first time step. During that time, the density of fully ionized carbon decreases by more than 42%, the electron density decreases by 9%, and the electron temperature decreases by 18%. The iterations still converge (although very slowly) if the time step is further increased by a factor two. There is no convergence, however, when $\Delta t$ becomes larger than approximately $250\mu s$. We note finally, that convergence is found empirically, to be relatively insensitive to the initial conditions assumed for the electron distribution function or for the distribution of ionisation stages. The main condition required for good convergence is that the macroscopic quantities such as the electron density and temperature, and the density of the dominant ionisation stages, should not vary too much (say by 15% or less) within a single time step.

## 4. Summary and Conclusions

A simple and efficient algorithm is presented for consistently modelling ionisation dynamics and electron kinetics in a plasma. The electron distribution function is governed by a Boltzmann equation which accounts for electron impact excitation and ionisation, together with radiative and dielectronic recombination. This equation and the ion rate equations are solved simultaneously and fully implicitly by iterations. For coronal plasmas, the method is found to be robust. It gives excellent convergence and charge conservation in only a few iterations provided that macroscopic parameters do not vary too rapidly in a single time step. Robustness and rapidity of convergence are often key issues, particularly when modelling mixtures of several ion species, or ions with large atomic numbers. In these cases, the time required to solve for atomic and electron kinetic processes can amount to a large fraction of the total simulation time. The iterative solution procedure proposed here can readily be extended to account for super elastic processes and three-body recombination, provided that these effects are sufficiently small to be treated perturbatively.

## Acknowledgments

The authors gratefully acknowledge financial support from the Atomic Energy of Canada Limited and the Natural Sciences and Engineering Research Council of Canada.

## References

1. C. J. Elliot and A. E. Greene, *J. Appl. Phys.* **47**, 2946 (1976).
2. A. R. Bell, R. Evans, and D. J. Nicholas, *Phys. Rev. Lett.* **46**, 243 (1981).

3. J. P. MATTE AND J. VIRMONT, *Phys. Rev. Lett.* **49**, 1936 (1982).
4. C. GORSE, M. CAPITELLI, J. BRETAGNE, AND M. BACAL, *Chem. Phys.* **93**, 1 (1985).
5. J. BRETAGNE, G. DELOUYA, C. GORSE, M. CAPITELLI, AND M. BACAL, *J. Phys. D* **18**, 811 (1985).
6. G. J. PERT, *J. Comput. Phys.* **39**, 251 (1981).
7. J. C. GAUTHIER, P. GEINDRE, N. GRANDJOUAN, AND J. VIRMONT, *J. Phys. D: Appl. Phys.* **16**, 321 (1983).
8. D. R. BATES, F. R. S. D'A. E. KINGSTON, AND R. W. P. MCWHIRTER, *Proc. R. Soc. London Ser. A* **267**, 297 (1962).
9. J. S. CHANG AND G. COOPER, *J. Comput. Phys.* **6**, 1 (1970).
10. K. L. BELL, H. B. GILBODY, J. G. HUGHES, A. E. KINGSTON, AND F. J. SMITH, *J. Phys. Chem. Ref. Data* **12**, 891 (1983).
11. R. A. HULSE, *Nucl. Technol. Fusion* **3**, 259 (1983).
12. R. M. MORE, *J. Quant. Spectrosc. Radiat. Transf.* **27**, 345 (1982).
13. R. MARCHAND, S. CAILLÉ, AND Y. T. LEE, *J. Quant. Spectrosc. Radiat. Trans.* **43**, 149 (1990).
14. M. N. ROSENBLUTH, W. M. MACDONALD, AND D. L. JUDD, *Phys. Rev.* **107**, 1 (1957).
15. L. SPITZER, JR., "The Physics of Fully Ionized Gases" (Interscience, New York, 1956).